© 2017. Published by The Company of Biologists Ltd | Journal of Cell Science (2017) 130, 152-163 doi:10.1242/jcs.180612

SPECIAL ISSUE: 3D CELL BIOLOGY

RESEARCH ARTICLE

Applied stretch initiates directional invasion through the action of Rap1 GTPase as a tension sensor

Spencer A. Freeman[1], Sonja Christian[2,3], Pamela Austin[3,4], Irene Lu[3,4], Marcia L. Graves[3,4], Lin Huang[5], Shuo Tang[5], Daniel Coombs[6], Michael R. Gold[2,3] and Calvin D. Roskelley[3,4,*]

ABSTRACT

Although it is known that a stiffening of the stroma and the rearrangement of collagen fibers within the extracellular matrix facilitate the movement of tumor cells away from the primary lesion, the underlying mechanisms responsible are not fully understood. We now show that this invasion, which can be initiated by applying tensional loads to a three-dimensional collagen gel matrix in culture, is dependent on the Rap1 GTPases (Rap1a and Rap1b, referred to collectively as Rap1). Under these conditions Rap1 activity stimulates the formation of focal adhesion structures that align with the tensional axis as single tumor cells move into the matrix. These effects are mediated by the ability of Rap1 to induce the polarized polymerization and retrograde flow of actin, which stabilizes integrins and recruits vinculin to preformed adhesions, particularly those near the leading edge of invasive cells. Rap1 activity also contributes to the tension-induced collective invasive elongation of tumor cell clusters and it enhances tumor cell growth *in vivo*. Thus, Rap1 mediates the effects of increased extracellular tension in multiple ways that are capable of contributing to tumor progression when dysregulated.

KEY WORDS: Mechanotransduction, Rap GTPases, Focal adhesions, Actin cytoskeleton, Talin, Vinculin, Integrin

INTRODUCTION

During the early stages of malignancy, remodeling of the tumor-associated extracellular matrix (ECM) increases stromal stiffening and realigns collagen fibers in an orientation perpendicular to the center of the tumor, both of which facilitate the outward migration of invasive tumor cells (Provenzano et al., 2006). Indeed, elevated tissue stiffness is a poor prognostic indicator in a number of cancers and stiffening of the ECM, on its own, can augment tumor cell invasion, demonstrating a direct link between these two processes (Levental et al., 2009; Lu et al., 2012; Paszek et al., 2005). Although stromal cells remodel tumor-associated matrices (Goetz et al., 2011), for tension to stimulate invasion it requires tumor cells to orient themselves in the direction of the realigned matrices. When applied to cells, tension impacts on a number of diverse processes including the orientation of cell–cell junctions and the cell division axis (Balachandran et al., 2011; Thery and Bornens, 2006; Thery et al., 2005; Tzima et al., 2005), and the maturation of focal adhesions that support cell migration (Paszek et al., 2005; Riveline et al., 2001). Because the cellular responses to stromal remodeling are complex, it is important to elucidate the mechanically sensitive signaling modalities that sense tensional changes and then influence tumor cell invasion.

Tumor cell invasion is coordinated by integrin-based focal adhesion complexes that couple the ECM to the actin cytoskeleton. The application of force to these complexes initiates conformational changes in a subset of focal adhesion proteins. For example, stretching individual talin molecules reveals otherwise cryptic binding sites for the adaptor protein vinculin (del Rio et al., 2009). Similarly, applying stretch to cellular exoskeletons stimulates the phosphorylation of a cryptic tyrosine residue within p130Cas (also known as BCAR1) (Sawada et al., 2006; Tamada et al., 2004). Once phosphorylated, p130Cas recruits a complex consisting of the Crk adaptor protein and C3G (also known as RAPGEF1), a guanine nucleotide exhange factor for Rap GTPases. C3G activates Rap GTPase when matrix-mediated stretch forces are applied to fibroblasts (Tamada et al., 2004) or when fluid-mediated shear forces are applied to hematopoietic cell lines (de Bruyn et al., 2003).

When in their active GTP-bound form, the Rap1 GTPases (Rap1a and Rap1b, each encoded by a separate gene but referred to collectively as Rap1) are major regulators of actin dynamics that act by binding multiple actin-regulatory proteins and recruiting them to the plasma membrane. Rap1-GTP binds Tiam1 and Vav2, both of which stimulate Arp2/3-based actin polymerization (Bos, 2005; Raaijmakers and Bos, 2009). Activated Rap1 also binds the RIAM (also known as APBB1IP) and AF6 (also known as MLLT4) adaptor proteins which recruit profilin, a protein that primes actin monomers for incorporation into actin filaments that are associated with maturing focal adhesions (Boettner et al., 2000; Lafuente et al., 2004). Additionally, Rap1 regulates the activity of cofilin (Freeman et al., 2011), an actin-severing protein that promotes actin polymerization as well as retrograde flow at the leading edge of migrating cells (Bravo-Cordero et al., 2013; Mouneimne et al., 2006). Because actin retrograde flow and actomyosin-based contractility both increase intracellular forces on nascent adhesions (Pasapera et al., 2010; Thievessen et al., 2013), Rap1 is a good candidate sensor of tensional changes in the ECM.

In this work, we show that the application of uniaxial stretch leads to anisotropic invasive membrane processes that extend along the tensional axis in multiple types of tumor cells. Our results reveal that the ability for individual cells to sense and respond to tension is dependent on Rap activation and the presence of talin. We demonstrate that Rap1 activation is important for the establishment of cell polarity, for the stabilization of integrins at the leading edge of the cell, and for changes in actin dynamics that promote the formation and maturation of focal adhesions. Taken together, our

[1]Program in Cell Biology, Hospital for Sick Children, Toronto, Ontario, Canada. [2]Department of Microbiology and Immunology, University of British Columbia, Vancouver, British Columbia, V6T 1Z3, Canada. [3]Life Sciences Institute, University of British Columbia, 2350 Health Sciences Road, Vancouver, British Columbia, V6T 1Z3, Canada. [4]Department of Cellular and Physiological Sciences, University of British Columbia, Vancouver, British Columbia, V6T 1Z3, Canada. [5]Department of Electrical Engineering, University of British Columbia, Vancouver, British Columbia, V6T 1Z3, Canada. [6]Department of Mathematics, University of British Columbia, Vancouver, British Columbia, V6T 1Z3, Canada.

*Author for correspondence (roskelly@mail.ubc.ca)

C.D.R., 0000-0003-0939-8900

Received 24 September 2015; Accepted 13 May 2016

Journal of Cell Science (2017) 130, 152-163 doi:10.1242/jcs.180612

findings suggest that the Rap GTPases sense tensional changes within the attached cell and selectively act on the actin cytoskeleton to initiate directional invasion along the axis of tension in three-dimensional (3D) matrices.

RESULTS

Applied uniaxial stretch to 3D matrices orients tumor cell invasion in the direction of the tensional axis

To test the ability of tumor cells to invade along a tensional vector, we made type I collagen gels containing fibronectin and applied a single 24-h-long phase of 10% uniaxial stretch (Fig. 1A). This was sufficient to reorient collagen fibers in the direction of the stretch, as determined by second harmonic imaging (Fig. 1A). We then cultured a wide range of normal and tumor-derived cell lines in the matrices before the application of tension in order to assess directional reorientation of the actin cytoskeleton once tension was applied. Extending anisotropic membrane processes into a matrix is thought to be a precursor to directional mesenchymal invasion (Parri and Chiarugi, 2010). To quantify this type of response, we fixed and stained cells for F-actin and calculated an invasive 'elongation factor' defined as the maximum length of the cell in the direction of applied tension divided by its maximum width in the perpendicular direction. The different cell lines exhibited a range of responses to the 24-h stretch (Fig. 1B). For example, epithelial MCF7 breast tumor cells exhibited an elongation factor close to 1 whereas mesenchymal MDA-MB-231 breast tumor cells exhibited an elongation factor of 3.25±1.69 (mean±s.e.m., n=100), reflecting substantial invasion into the matrix along the axis of tension (Fig. 1B).

As the physical characteristics of the matrix are known to affect focal adhesion formation (Fraley et al., 2010; Geiger and Yamada, 2011), we subsequently stained cells that responded to the uniaxial stretch for the focal adhesion protein vinculin. We found that cells embedded in relaxed matrices formed small vinculin-containing focal-contact-like structures, whereas those in tensed matrices formed adhesion plaques with a threefold to fivefold increase in vinculin enrichment (Fig. 1C). The focal adhesions that formed in tensed 3D matrices were also elongated in the direction of applied stretch and strongly localized to the ends of F-actin stress fibers (Fig. 1C). Invasion along the axis of tension resulted in the formation of focal adhesions and also required their assembly. Upon knocking down the expression of talin 1 and talin 2 (Fig. 1D), integrin-binding proteins that also mediate cytoskeletal linkage, single tumor cells showed a significantly reduced elongation factor despite having some actin-rich invasive processes (Fig. 1E). Taken together, these observations indicate that tension applied through 3D matrices reorients some tumor cell types through signals that are transduced by the ECM.

Acute stretch activates Rap1 in tumor cells

In endothelial cells, reorientation in response to shear stress or tension has been shown to require cell shape change governed by Rho GTPases, which control actin polymerization (Abiko et al., 2015; Hahn et al., 2011; Wojciak-Stothard and Ridley, 2003). To determine the signaling pathways activated in tumor cells that regulate the actin cytoskeleton in response to applied tension, we required an experimental system where cells could be readily lysed and subjected to biochemical analyses. We therefore utilized two-dimensional (2D) fibronectin-coated silicone rubber substrata and exerted equibiaxial stretch to maximize the exogenous tensional force applied to the cells. As was the case for cells in 3D matrices, tension applied in this manner also increased the amount of vinculin associated with adhesions, although without directional preference (Fig. 2A). The ratio of the vinculin signal to integrin signal showed a twofold increase upon 10 min of equibiaxial stretch (Fig. 2A). As previously determined in fibroblasts (Sawada et al., 2006), the application of acute tension also increased the phosphorylation of the adhesion plaque molecule p130Cas at tyrosine 165. This was observed within 5 min of initiating stretch (Fig. 2B). We then assessed the activation of the Rap1, RhoA and Rac1 GTPases, major regulators of the actin cytoskeleton (Collins et al., 2012; Mammoto et al., 2004; Provenzano and Keely, 2011) and found that the equibiaxial stretch described above rapidly and strongly activated Rap1 within 2 min (Fig. 2C,D). In contrast, there was a small, but statistically significant increase, in RhoA activation and no measurable increase in Rac1 activation (Fig. 2D). Therefore, we next assessed the functional importance of Rap1 activation in the invasion response of tumor cells in 3D matrices.

The activation of Rap1 is necessary for stretch-induced formation of focal adhesions in 3D matrices and directional invasion

To increase Rap1 activation in B16F1 melanoma cells, we expressed the constitutively active Rap1V12 protein (Freeman et al., 2010) and then compared focal adhesions in cells that were in relaxed versus uniaxially stretched 3D matrices. B16F1 cells stably expressing Rap1V12 formed vinculin-rich focal adhesions even in the absence of applied tension (Fig. 3A). Strikingly, when tension was applied, these focal adhesions oriented along the tensional axis but did not recruit more vinculin (Fig. 3A,B). This suggests that either Rap1V12 causes maximal association of vinculin at adhesions, which cannot be increased further by tension, or that tension-induced vinculin loading is mediated entirely by Rap1.

To test the idea that exogenous stretch activates Rap1 and that this stimulates vinculin recruitment to adhesions, we blocked Rap activation either by expressing the functional inhibitor Rap1GAPII (also known as RAP1GAP2) or by knocking down. Both of these approaches completely ablated the stretch-induced recruitment of vinculin to adhesions as well as the anisotropic invasive membrane processes of the cells in 3D gels (Fig. 3A–C,E,F). This was not due to changes in the expression of adhesion proteins such as talin and vinculin (Fig. S1) and therefore most likely reflects differences in the assembly of vinculin at adhesions.

As another measure of the tensional response to altered Rap activity, we cultured cells in collagen and released the gels after 48 h to determine the extent of contraction. We found that expression of the constitutively active Rap1V12 protein increased the ability of the cells to contract the gels by twofold compared to control cells, whereas blocking Rap activation by expressing Rap1GAPII ablated contraction altogether (Fig. 3D). These observations strongly suggest that stretch-induced Rap activation translates tension that is applied externally through the ECM into an intracellular increase in tension that acts through focal adhesions to contract the gel.

Rap activation and actin polymerization at the leading edge of the cell establishes a gradient of vinculin-rich focal adhesions that are under tension

Because vinculin-enriched focal adhesions formed at the invasive front of cells in 3D matrices in both a Rap1- and a tension-dependent manner, we assessed the connection between Rap activation and the stretch-mediated recruitment of vinculin to focal adhesions. Rap1 is a major regulator of actin polymerization (Raaijmakers and Bos, 2009), which is a requirement for vinculin to localize to focal adhesions. Indeed, we found that the brief pharmacological inhibition of actin polymerization by treating

Journal of Cell Science (2017) 130, 152-163 doi:10.1242/jcs.180612

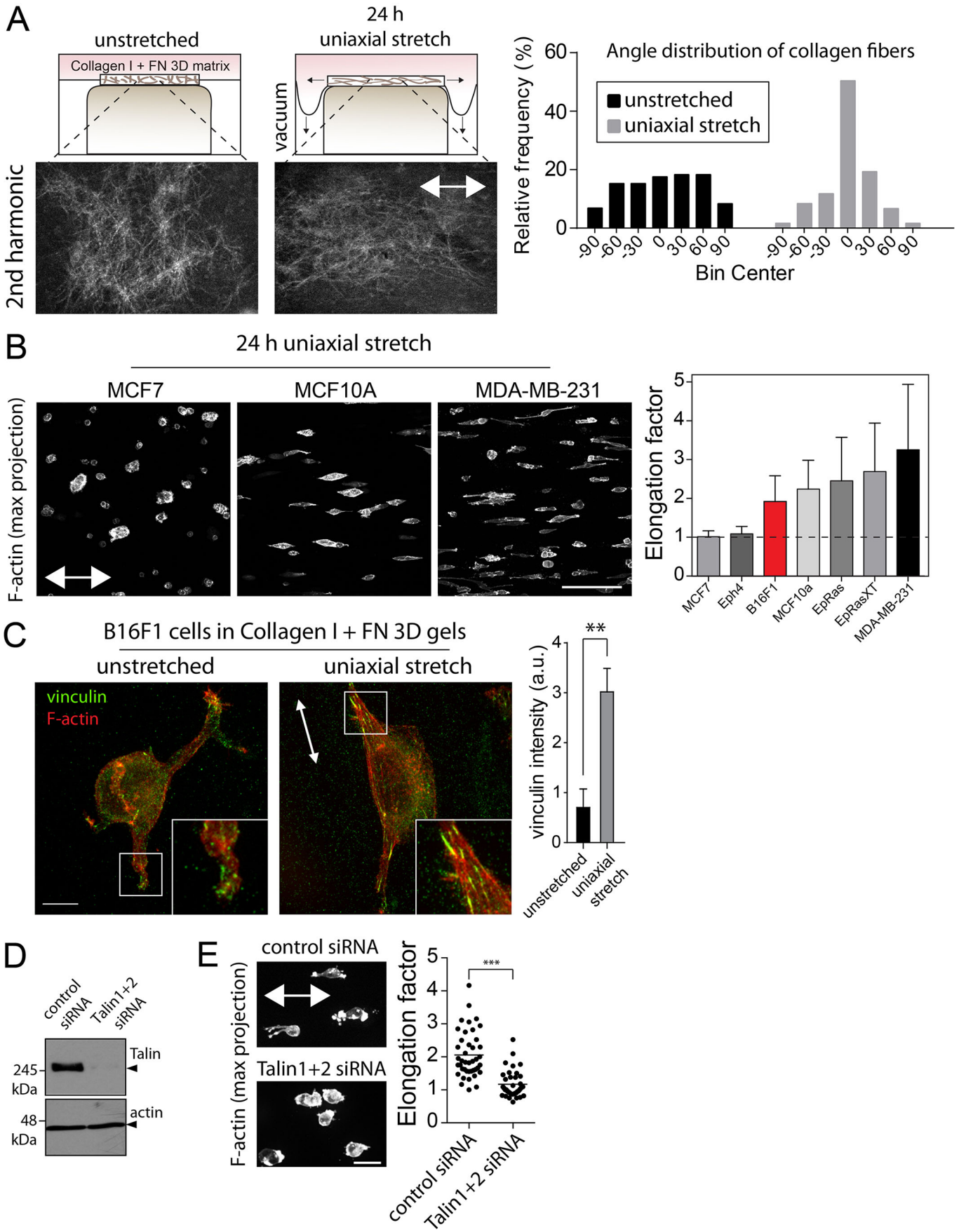

Fig. 1. See next page for legend.

Journal of Cell Science (2017) 130, 152-163 doi:10.1242/jcs.180612

Fig. 1. Tumor cells form focal adhesions and invade 3D collagen-containing gels in a directional manner in response to uniaxially applied tension. (A) Collagen I (2.17 mg/ml)+fibronectin (FN, 5 µg/ml) 3D gels were polymerized and either left unstretched or uniaxally stretched for 24 h and then imaged by second harmonics. White arrows indicate the direction of applied stretch. Fiber orientation is quantified by measuring >100 fibers from two experiments and is graphed (below). (B) Indicated cell lines were seeded within 3D collagen I+fibronectin gels and stretched for 24 h. An elongation factor for the cells was determined by staining for F-actin and measuring the maximum length along the tensional axis divided by the maximum width of the perpendicular axis. Bars represent the mean±s.d. from >50 cells from at least two experiments. Scale bar: 100 µm. (C) B16F1 cells in relaxed or uniaxially stretched gels were fixed and stained for F-actin and vinculin. Images shown are from *z*-stacks projected through the *xy* plane (left). Scale bar: 10 µm. The total intensity per cell of vinculin staining at adhesions in arbitrary units (a.u.) was calculated from *z*-stacks and the mean±s.e.m. (n>30 cells) is shown. (D,E) B16F1 cells that were transfected with either scrambled control siRNA or talin1 plus talin2 siRNAs were assessed for talin expression by western blotting (D) and for elongation in 3D collagen (E) as in B. Scale bar: 50 µm. $^{**}P$<0.005, $^{***}P$<0.001 (paired two-tailed Student's *t*-tests).

cells with latrunculin A (latA) decreased the ratio of vinculin:β1 integrin at adhesions (Fig. 4A), even when cells were under equibiaxial stretch. Actin polymerization could regulate vinculin loading at adhesions in two ways. First, myosin II, which is associated with actin filaments that are connected to adhesions, could contract the filaments and produce intracellular forces on talin to reveal vinculin-binding sites (Margadant et al., 2011; Pasapera et al., 2010). Alternatively, newly polymerized actin at the leading edge of cells could generate force at adhesions by traversing over them by retrograde flow.

To explore the possibility that applied tension causes Rap1-dependent actomyosin contraction, we applied equibiaxial stretch to cells plated on fibronectin-coated silicone rubber substrata and assessed the phosphorylation of myosin light chain II (MLCII, also known as MYL2), which is required for myosin II activation. We found that the level of phosphorylated MLCII remained constant in the cells during stretch, and that this steady-state level was maintained independently of Rap1 activation (Fig. S1). We noted that when the cells were spread on fibronectin, the level of phosphorylated MLCII did increase, but that this was also independent of Rap activation (Fig. S1). Previous studies have demonstrated that myosin II activity leads to increased phosphorylation of paxillin (Pasapera et al., 2010) and we found this was also independent of Rap activation (Fig. S1). Furthermore, increasing Rap1 activation by expressing Rap1V12 did not increase the amount of phosphorylated MLCII bound to actin filaments (Fig. S1), suggesting that Rap1 does not regulate myosin II or promote myosin-based contractility.

We next tested the second possibility, that Rap1-GTP stimulates actin polymerization at the leading edge of the cell and that the resulting retrograde flow of actin promotes the recruitment of vinculin to adhesions. A biosensor for active Rap (RapL–GFP), was used to demonstrate that Rap-GTP localized to the leading edge where actin polymerization occurred (Fig. S2). We then reasoned that if the retrograde flow of newly polymerized actin networks promotes vinculin loading at focal adhesions, there should be an inverse relationship between the sites of vinculin loading and their distance from the leading edge of the cell where Rap-GTP localizes and stimulates actin polymerization. To test this, we took advantage of the fact that B16F1 cells spontaneously polarize on 2D substrata, which makes it possible to readily determine the spatial relationship between vinculin and the leading edge. Remarkably, we found a linear relationship between the vinculin:β1 integrin ratio at adhesions of and the distance of the adhesion from the leading edge of the cell (Fig. 4B,C). The adhesions that formed closest to the leading edge (i.e. within 0–2.5 µm) had the highest amount of vinculin relative to β1 integrin (Fig. 4B; Fig. S3). Blocking Rap activation through Rap1GAPII expression decreased the vinculin:β1 integrin ratio at all adhesions, but this was particularly apparent for the adhesions that formed closest to the edge of the cell (Fig. 4C). Upon acute application of equibiaxial stretch, the vinculin:β1 integrin ratio increased at all adhesions in a Rap- and actin-dependent manner (Fig. 4A–C). These results show that, on relaxed substrates, vinculin preferentially accumulates at focal adhesions behind the leading edge in an actin- and Rap-dependent manner, and that upon stretch, adhesions further behind the leading edge become enriched in vinculin through a mechanism that requires Rap activation (Fig. 4C).

Once vinculin binds to talin at focal adhesions, it can undergo tension-mediated stretching and straightening, a process that is regulated by the actin cytoskeleton and which can be detected using a FRET-based tension sensor for vinculin (Grashoff et al., 2010). Expressing this vinculin tension sensor in B16F1 cells showed that vinculin in Rap1V12-expressing cells, and at the leading edge of control cells, was under high tension, as indicated by the low FRET signal (Fig. S3). Importantly, when Rap activation was blocked by Rap1GAPII expression, the rare vinculin-rich adhesions that remained were under low tension, as indicated by a high FRET signal at these adhesions (Fig. S2). Thus, Rap activation is important for both the initial loading of vinculin at adhesion complexes and for the subsequent generation of tension that is sensed by vinculin at these complexes.

Rap1 activation establishes a polarized distribution of actin polymerization, PI3K signaling and Rac1 activation at the leading edge

Because both Rap activation and actin are required for focal adhesion assembly and vinuclin loading at the leading edge of the cell, we asked whether Rap1 coordinates these responses by promoting actin polymerization. To test this we used fluorescence recovery after photobleaching (FRAP) to assess the rate at which actin-GFP is assembled into filaments in control versus Rap1GAPII-expressing B16F1 cells. Control cells plated on fibronectin-coated tissue culture plastic exhibited an accumulation of β-actin–GFP in broad actively ruffling leading edges. Upon bleaching the β-actin–GFP, the fluorescence signal recovered rapidly at the leading edge of the cell, progressing in a retrograde direction from the plasma membrane towards the cell body (Fig. 5A). The post-bleaching recovery of β-actin–GFP fluorescence was greatly reduced in cells in which Rap activation was blocked by expressing Rap1GAPII (Fig. 5A). This indicates that Rap activation stimulates actin polymerization at the polarized, leading edge of the cell.

Actin nucleation at the leading edge is stimulated by the Arp2/3 complex and nucleation-promoting factors that are activated by small Rho GTPases. Rap is a major regulator of cell polarity in part because its active form binds to GEFs that activate the Rac and Cdc42 GTPases. Rap1 might also bind phosphoinositide 3-kinase (PI3K) and recruit it to the plasma membrane, where it generates the lipid second messenger phosphatidylinositol (3,4,5)-trisphosphate (PIP_3) (Kortholt et al., 2010). By serving as a ligand for PH-domain-containing proteins, PIP_3 recruits activators of the Rac and Cdc42 GTPases to the plasma membrane. Thus, PI3K is a key upstream activator of GTPases that control cytoskeletal dynamics and organization. By using the PIP_3 biosensor, the PH domain of Akt

Journal of Cell Science (2017) 130, 152-163 doi:10.1242/jcs.180612

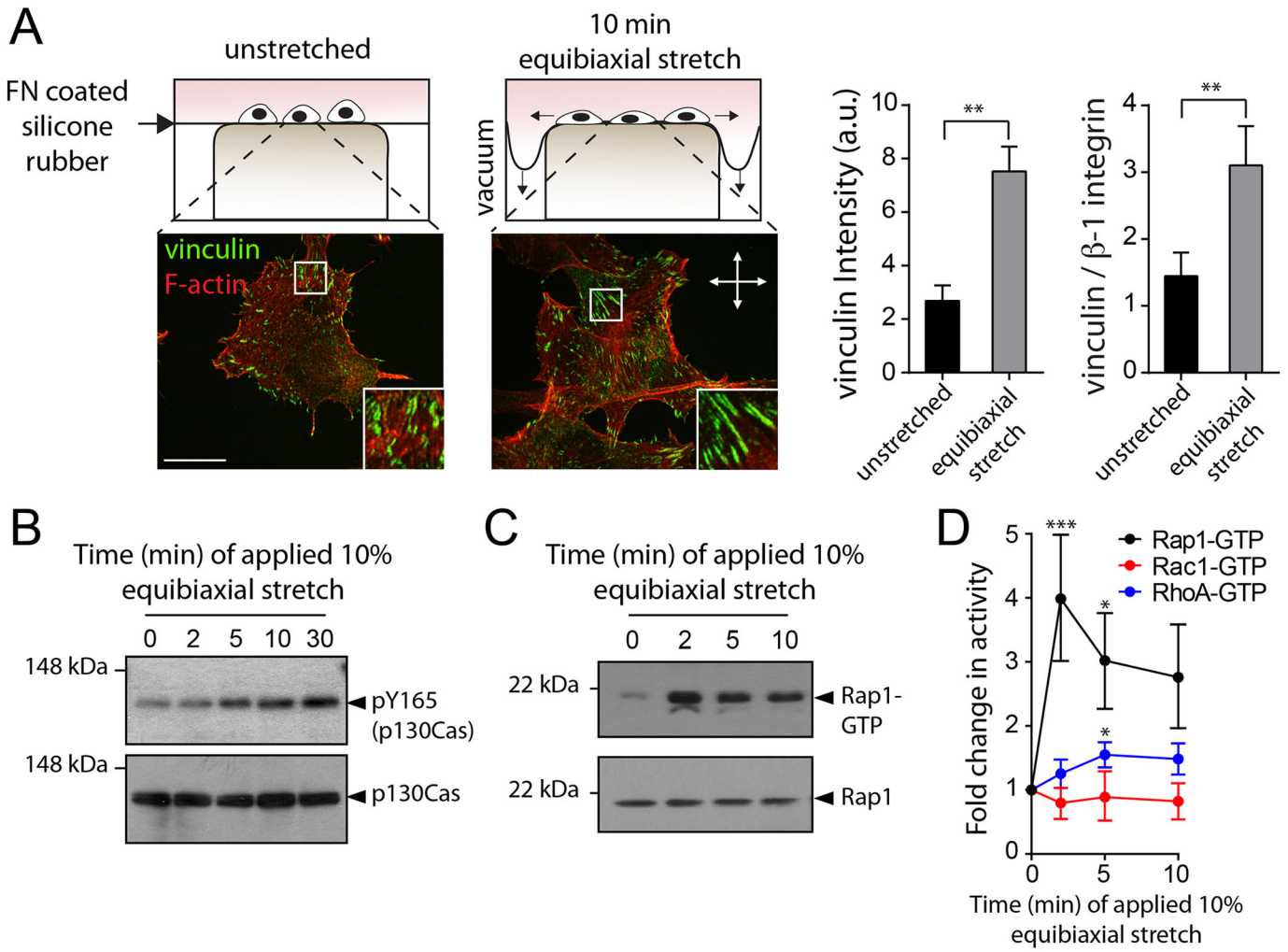

Fig. 2. Applied stretch stimulates vinculin binding at focal adhesions, p130Cas phosphorylation and Rap activation. (A–D) B16F1 cells were seeded onto fibronectin-coated (5 µg/cm^2) silicone rubber plates overnight before applying 10% equibiaxial stretch to the substrata for indicated times. (A) Cells were stained using vinculin antibodies and Rhodamine–phalloidin to visualize F-actin (left panels). Total vinculin intensity at adhesion complexes was quantified for unstretched control cells as well as stretched cells (left graph) and normalized to β1 integrin intensity (right graph). *n*>30 cells from three independent experiments. Scale bar: 10 µm. (B) Phosphorylation of Y165 in p130Cas was probed using phospho-specific antibodies. Total p130Cas is shown below. (C) The amount of active Rap1 (Rap1-GTP) was determined by performing a Ral-GDS-GST pulldown and probing with anti-Rap1 antibodies. Total Rap1 from a fraction of the lysates is shown below. (D) The levels of active GTP-bound Rac1 and RhoA were determined using G-LISA assays. Rap1, Rac1, and RhoA activities were normalized to time 0 (pre-stretch) samples. The mean±s.e.m. from three experiments is graphed. **P*<0.05, ***P*<0.005, ****P*<0.001 (unpaired two-tailed Student's *t*-tests).

fused to GFP, and a FRET-based sensor for Rac1 activation, we found that as cells assumed a polarized phenotype on 2D ECMs, and that PIP_3 and active Rac1 accumulated at the leading edge. Blocking Rap activation, either by expressing either Rap1GAPII or a dominant-negative form of Rap1 (Rap1N17), reduced the accumulation of PIP_3 and activated Rac1 at the plasma membrane and, importantly, abrogated the polarization of PIP_3 and activated Rac1 (Fig. 5B,C). Together with our finding that activated Rap is enriched at the leading edge of the cell (Fig. S2), these data support the idea that localized Rap activation stimulates PIP_3 production and Rac1 activation, leading to polarized actin polymerization at the leading edge of the cell.

Rap1 activity is required for the tension-induced stabilization of integrins

Up to this point, we have demonstrated that applied tension activates Rap GTPases to stimulate the actin polymerization that orients tumor cell invasion along the tension axis. Although Rap1 is required for polarization of the cells, it remains unclear how adhesions themselves become oriented and then stabilized along the axis of tension. To directly determine whether the dynamics of proteins moving in and out of focal adhesions is altered by changes in tension, we utilized a system in which the adhesions could be photobleached throughout the process. Silicone rubber, although an excellent substrate to apply stretch to cells, cannot be penetrated by conventional confocal microscopy. We therefore plated cells on fibronectin-coated tissue culture plastic within flow chambers where we could reversibly apply shear flow, a system used in other studies to reorient cell monolayers (Tzima et al., 2005). We confirmed that fluid-based shear flow caused a rapid increase in Rap1-GTP levels in B16F1 cells (Fig. 6A), demonstrating that the tension sensor is also sensitive to shear.

To assess the effects of external forces on adhesion dynamics, cells expressing α5-integrin–GFP were plated on fibronectin-coated tissue culture plastic for 2–4 h to allow adhesions to form. FRAP was then used to assess the effects of shear flow on adhesion

Journal of Cell Science (2017) 130, 152-163 doi:10.1242/jcs.180612

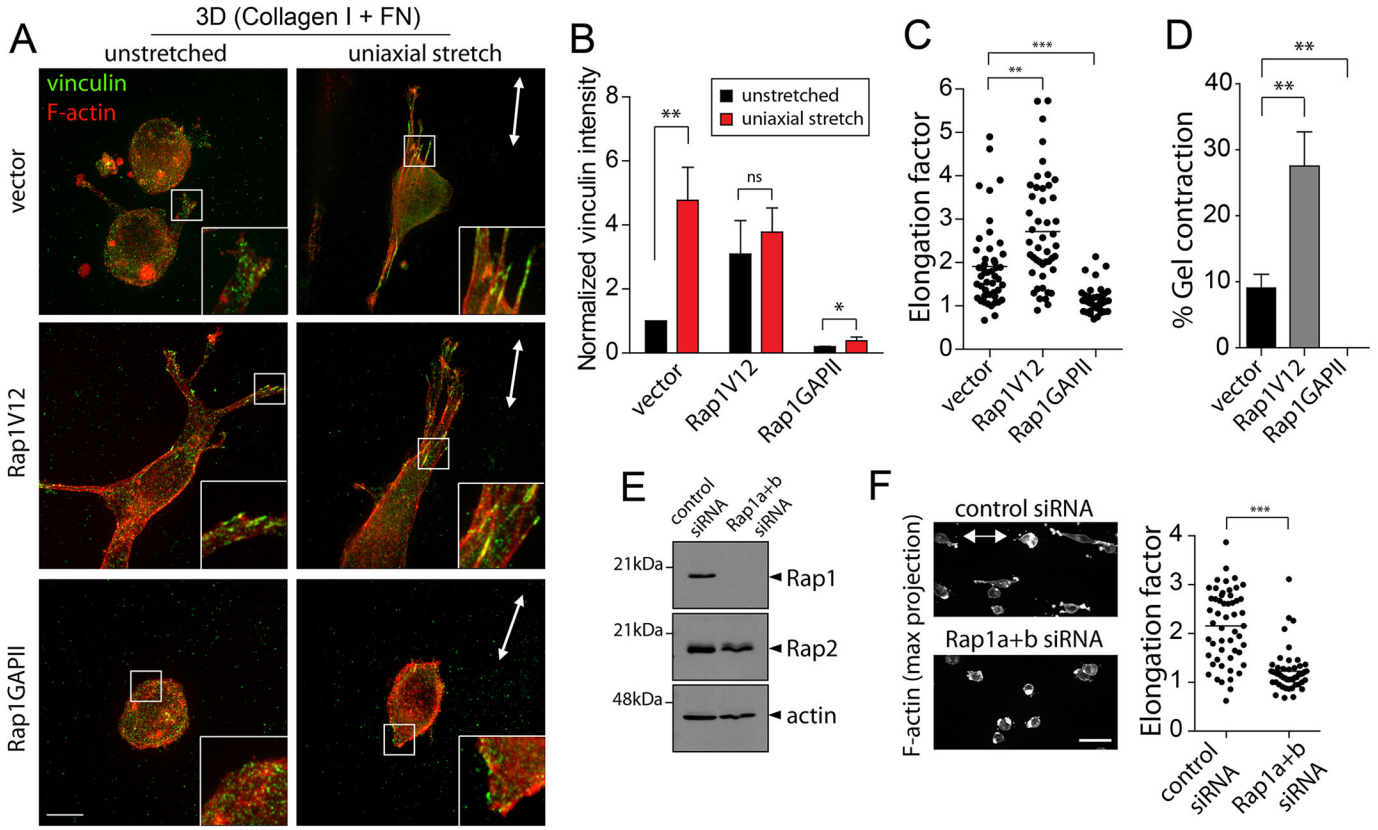

Fig. 3. Tension-induced focal adhesion formation and tumor cell invasion are dependent on Rap activation. (A,B) B16F1 cells stably expressing empty vector, Rap1V12 or Rap1GAPII were seeded within 3D collagen I+fibronectin (FN) gels and stretched for 24 h. Vinculin fluorescence is shown (A) and quantified (mean±s.e.m., *n*>30 cells; B). Scale bar: 10 µm. White arrows indicate the direction of applied stretch. (C) The elongation factor for >40 cells from three experiments was determined. (D) B16F1 cells stably expressing vector, Rap1V12 or Rap1GAPII were cultured in collagen gels and released to determine the percentage contraction compared to gels without cells added. The mean±s.e.m. from three experiments is graphed. (E,F) B16F1 cells transfected with either scrambled control siRNA or Rap1a plus Rap1b siRNAs were assessed for the expression of Rap1, Rap2 and β-actin by immunoblotting (E), and for elongation in 3D collagen gels (F). Scale bar: 50 µm. **P*<0.05, ***P*<0.005, ****P*<0.001 (paired two-tailed Student's *t*-tests).

dynamics. Fluorescence recovery of α5-integrin–GFP within a region of interest (ROI) was recorded after applying a shear flow of 20 dynes (blue lines), and then after terminating the shear flow (red lines) (Fig. 6B,C). Applying shear reversibly changed the extent of fluorescence recovery for α5 integrin, indicating changes in adhesion dynamics. The application of shear forces decreased the maximal fluorescence recovery of α5-integrin–GFP from 25% to 15% in fibroblasts and from 42% to 27% in B16F1 cells, presumably reflecting increased stabilization of fibronectin binding in response to the increase in resulting intracellular tension (Fig. 6B).

In line with our previous findings using stretch to induce intracellular tension, activating Rap1 was sufficient to induce focal adhesion phenotypes normally observed under the application of shear force. Specifically, the expression of Rap1V12 in B16F1 cells decreased the maximal fluorescence recovery of α5-integrin–GFP to the same extent as shear (compare Rap1V12, blue dots, to vector, red dots, Fig. 6C). Integrin turnover in Rap1V12-expressing B16F1 cells was further modulated to a modest extent by shear forces, but to a much lesser degree than in vector control cells.

To quantify the effects of Rap activation on focal adhesion dynamics, we used differential-equation-based models to derive the turnover kinetics parameters k_{on} and k_{off} from the FRAP curves of α5-integrin–GFP (Pines et al., 2012; Wolfenson et al., 2011). We found that expressing Rap1V12 increased the k_{on} for α5 integrin from 0.052 to 0.063 s^{-1} and reduced the k_{off} for α5 integrin from 0.039 to 0.025 s^{-1} (Fig. 6C), suggesting that both parameters are Rap1 dependent.

Prior to ECM binding and adhesion complex formation, the Rap GTPases facilitate the recruitment of talin to integrin β subunits, promoting conversion of the integrin heterodimer to an activated form that can bind ECM ligands (Han et al., 2006). To rule out the possibility that the changes in integrin dynamics within pre-existing adhesions were simply due to activation of the integrin, we expressed a mutant form of the β1 integrin subunit (G429N) that constitutively forces the integrin heterodimer into an extended active form (Rubashkin et al., 2014). Within pre-existing adhesions, this mutant β1 integrin subunit exhibited the same fluorescence recovery after photobleaching as the wild-type integrin (Fig. 6D). This supports the idea that activated Rap1 regulates adhesion component dynamics within pre-existing adhesions by mechanisms other than promoting integrin activation.

Rap1 activation is not required for cell–cell junction reorientation

Tumor cells can invade the local stromal as single cells, but frequently do so by collectively pushing into the matrix as an elongated structure (Bronsert et al., 2014). Collective tumor cell invasion maintains cell–cell adhesion while cells at the invasive front adhere to the ECM. In this scenario, cells at the invasive front assume a polarized phenotype with a leading edge whereas trailing cells

Journal of Cell Science (2017) 130, 152-163 doi:10.1242/jcs.180612

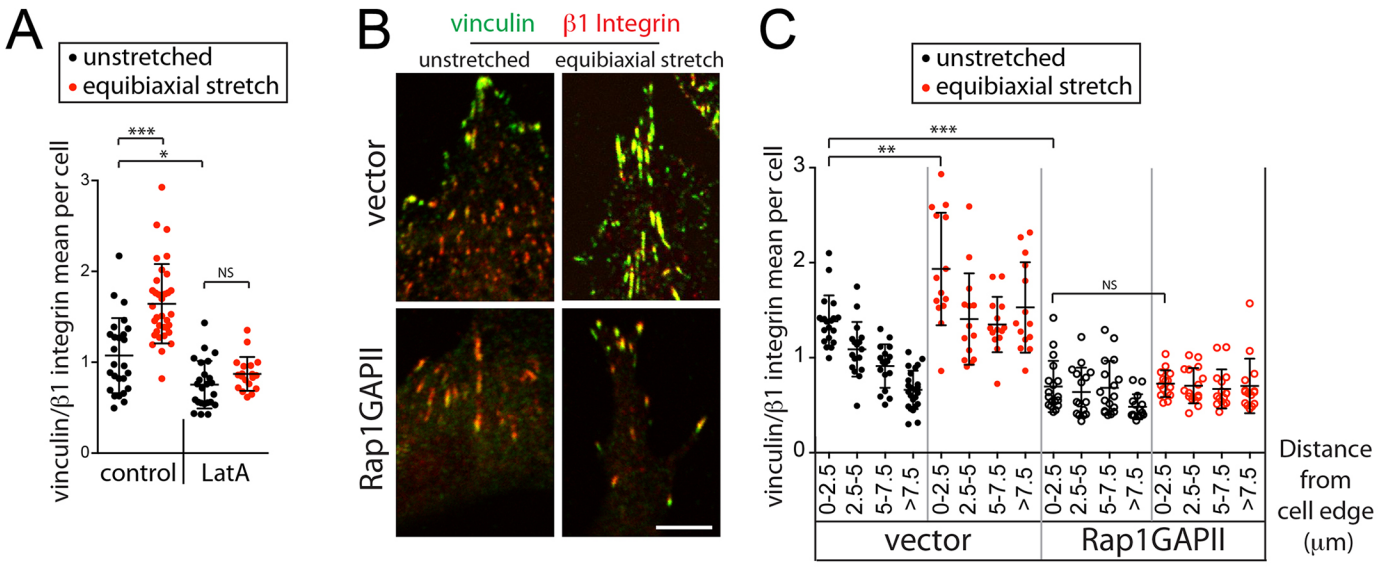

Fig. 4. Stretch-induced recruitment of vinculin to focal adhesions near the leading edge requires Rap activation and actin polymerization. (A) B16F1 cells were cultured on fibronectin-coated (2.5 µg cm^{-2}) silicone rubber plates overnight before applying 10% equibiaxial stretch to the substrata for 10 min. Cells were treated with or without 1 µM latrunculin A for the last 3 min of applied stretch, fixed and stained for vinculin and β1 integrin. The ratio of vinculin intensity to β1 integrin intensity per adhesion was quantified for >20 cells from three experiments and graphed. Only adhesions at the leading edge were quantified. (B,C). B16F1 cells transiently expressing the empty vector or Rap1GAPII–FLAG were plated on fibronectin-coated silicone rubber plates overnight before applying 10% equibiaxial stretch to the substrata for 10 min where indicated. Cells were fixed and stained for vinculin and β1 integrin (B). The ratio of vinculin to β1 integrin intensities per adhesion was quantified for >15 cells from three experiments and graphed according to the distance from the leading edge of the cell (C). See also Fig. S1. Scale bar: 2 µm. **P*<0.05; ***P*<0.01; ****P*<0.001; NS, not significant (unpaired two-tailed Student's *t*-tests).

maintain cell–cell junctions. The effect of externally applied tension on collective invasion has not been assessed. We therefore asked whether tumor cell masses that maintain cell–cell adhesion elongate in the axis of tension in the same manner as single cells (see Fig. 1). To test this, we seeded B16F1 cells into 3D collagen gels and kept the matrices under tension for 48 h. During this period, the tumor cells began to divide and largely grew as small clusters of cells rather than breaking away and invading the ECM singly. Under these conditions tumor cell clusters invaded in an elongated manner along the axis of tension and this was dependent on Rap activation (Fig. 7A). Under tension, actin-rich cell–cell junctions became oriented perpendicular to the axis of tension and surprisingly this was not altered when Rap activation was blocked (Fig. 7A,B). Indeed, in both vector control and Rap1GAPII-expressing cells the distribution of the angle of cell–cell junctions relative to the axis of tension assumed a Gaussian distribution centering near 90°. Thus, whereas tension-dependent focal adhesion alignment is Rap dependent, tension-dependent alignment of cell–cell junctions is not.

Rap1-GTP regulates B16F1 melanoma cell growth in 3D matrices and *in vivo*

The formation of vinculin-containing focal adhesions in 3D matrices is important for tumor cell growth and invasion (Rubashkin et al., 2014). Because Rap-dependent focal adhesion formation in 3D collagen persisted for at least 5 days (Fig. S4), we asked whether modulating Rap activation controlled B16F1 cell growth. In 3D collagen matrices, constitutive activation of Rap1 increased colony volume by twofold whereas blocking Rap activation decreased the volume by 50% (Fig. S4). The change in growth under these low-tension conditions was likely a result of integrin stabilization (see Fig. 6), increased focal adhesion formation and vinculin loading (see Figs 3 and 4), and, presumably, increased focal-adhesion-based signaling. In contrast, control, Rap1V12-expressing and Rap1GAPII-expressing cells exhibited similar growth kinetics on rigid 2D tissue plastic, which would generate high intracellular tension (Fig. 7C). Thus, Rap1-dependent effects on tumor cell growth are only apparent under conditions in which focal adhesion formation is most susceptible to changes in Rap1 activity (i.e. under low to moderate tension). Because tumor growth *in vivo* in the context of compliant tissue structures represents a condition of low to moderate tension, we asked whether Rap activation altered the ability of tumor cells to grow *in vivo*. Indeed, blocking Rap activation reduced the growth of B16F1-cell-derived subcutaneous tumors in mice (Fig. 7D). Thus, the ability of Rap to sense extracellular tension and translate this into changes in adhesion dynamics appears to be a regulator of *in situ* tumor growth as well as invasion.

DISCUSSION

We report that the application of tension across 3D matrices initiates the directional invasion of single tumor cells and cohesive tumor cell clusters along the axis of applied tension. Both forms of invasion are dependent on signals from the ECM that increase the activation of Rap1 in the cells. In turn, Rap1-GTP is required for tumor cells to stabilize integrin contacts with the ECM, form bona fide focal adhesions in the matrices that recruit vinculin, and reorient their actin cytoskeleton to elongate in the axis of tension (see model in Fig. 7E). In contrast, the ability of cells to reorient their cell–cell junctions in response to the increased tension does not require Rap activity, suggesting that there are some tension-sensitive signaling pathways that can influence cytoskeletal remodeling independently of Rap1. In support of this notion, we also found that the tension-induced phosphorylation of p130Cas and paxillin, as well as the activation of myosin II, are all Rap1-independent. These findings point to a complex interplay between Rap1-dependent and -independent processes in the initiation of directional invasion.

Journal of Cell Science (2017) 130, 152-163 doi:10.1242/jcs.180612

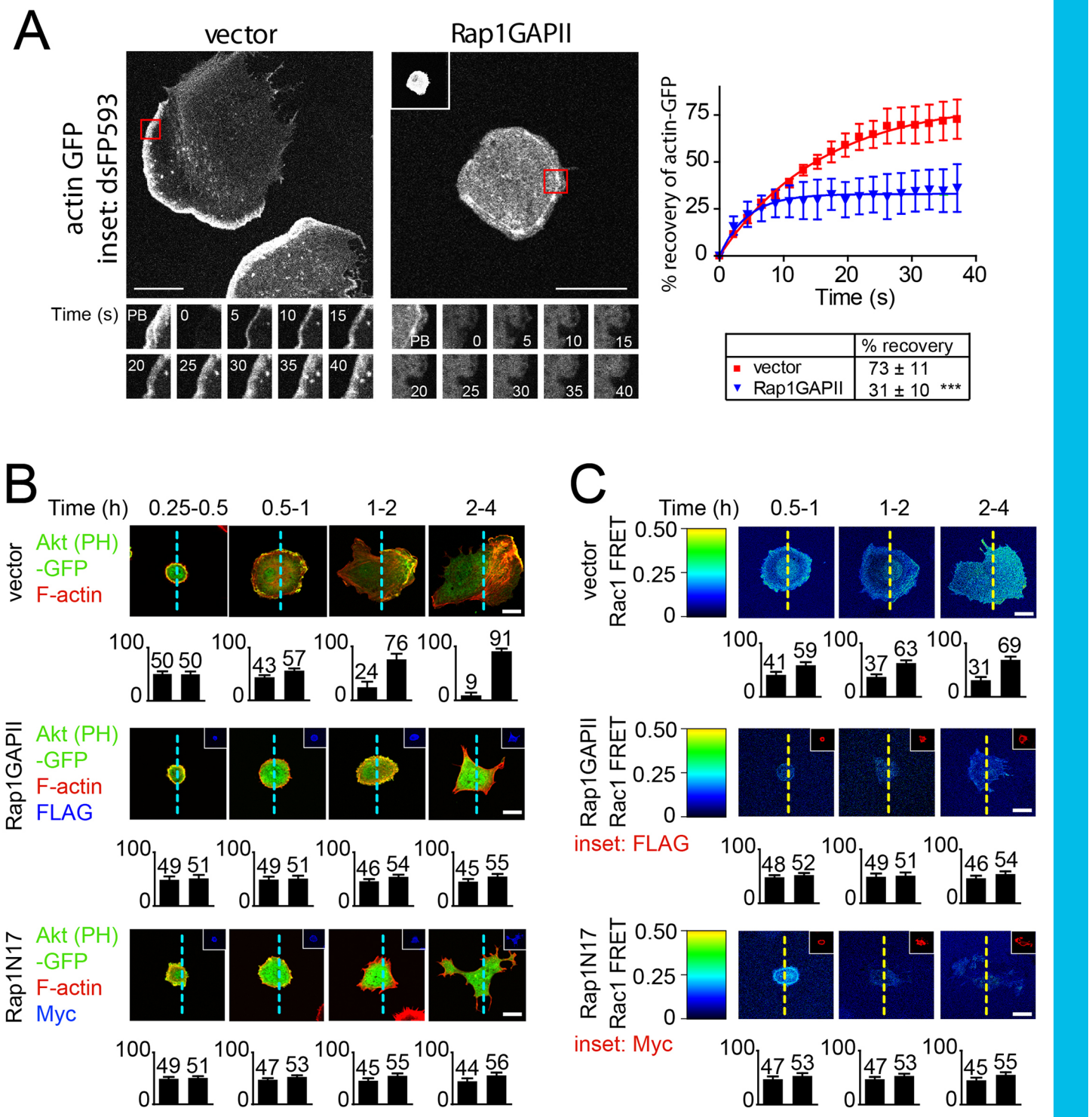

Fig. 5. Rap activation is required for actin polymerization as well as PIP_3 accumulation and Rac1 activation at the leading edge of tumor cells. (A) B16F1 cells were transfected with actin–GFP plus either Rap1GAPII or an empty vector and then seeded onto fibronectin-coated (2.5 µg cm^{-2}) chamber slides for 2 h. Peripheral actin structures were photobleached and the recovery of fluorescence was determined over at least 30 s. Examples are shown in left panels. The mean±s.e.m. of the percentage recovery of actin-GFP for >30 cells from three experiments is graphed. PB, pre-bleach. Scale bars: 10 µm. ***P<0.001 (paired two-tailed Student's t-tests). (B,C) B16F1 cells were transiently transfected with vector, Rap1GAPII–FLAG or Rap1N17-Myc and either Akt (PH)–GFP or Raichu-Rac1 before being plated on fibronectin-coated (2.5 µg/cm^2) coverslips for the indicated times. (B) Cells were fixed and stained for FLAG or Myc to identify transfected cells. F-actin was visualized using Rhodamine–phalloidin and the amount of co-localized Akt(PH)–GFP and F-actin was quantified. Cells were divided into two equal regions (as indicated by the dotted lines), corresponding to leading and trailing edges when these were present, and the amount of colocalized Akt(PH)–GFP and F-actin in each half of the cell was determined. In each graph, the bars on the left represent the trailing part of the cell and the bars on the right represent the leading part of the cell. The mean±s.e.m. for 30 cells from three experiments is graphed and the numbers above each bar is the mean value. (C) Cells were fixed and stained for FLAG or Myc and the amount of activated Rac1 in each half of the cell, as indicated by the FRET intensity of the Raichu-Rac1 fusion protein, was determined by measuring the CFP fluorescence before and after bleaching YFP. FRET intensity in the trailing (left bars) and leading (right bars) parts of the cell are graphed (mean±s.e.m.). n=30 cells from 3 experiments. Scale bars: 10 µm.

Journal of Cell Science (2017) 130, 152-163 doi:10.1242/jcs.180612

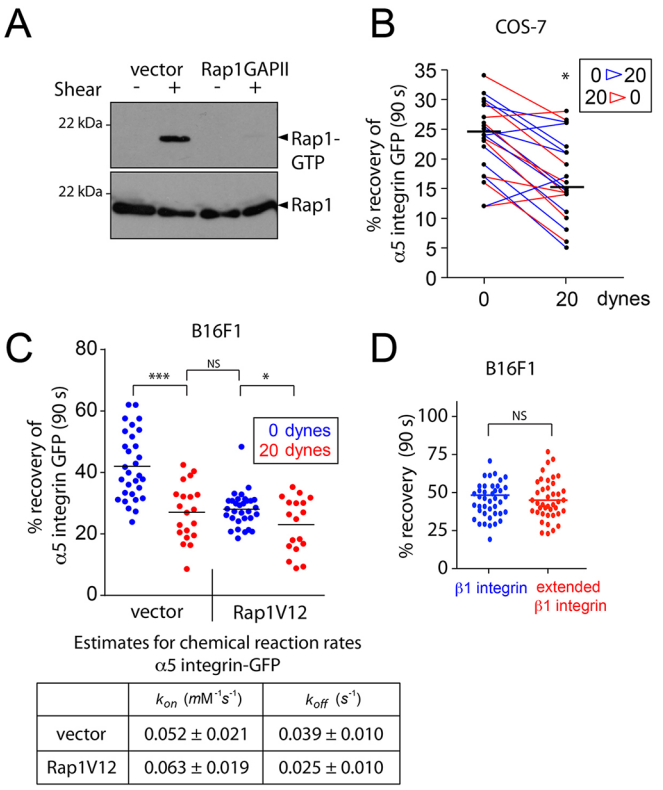

Estimates for chemical reaction rates α5 integrin-GFP

	k_{on} ($mM^{-1}s^{-1}$)	k_{off} (s^{-1})
vector	0.052 ± 0.021	0.039 ± 0.010
Rap1V12	0.063 ± 0.019	0.025 ± 0.010

Fig. 6. Acute shear flow activates Rap1 to stabilize integrins at established focal adhesions. (A) B16F1 cells were resuspended in DMEM and either lysed or passed through a 28 G needle for 2 min. The amount of Rap1-GTP in cell lysates was assessed by western blotting. (B) For FRAP analysis, COS-7 cells were transfected with α5-integrin–GFP and seeded onto fibronectin-coated flow chamber slides. A syringe was used to draw medium from the end of the chamber, creating a 20-dyne shear force that could be rapidly turned on or terminated. Adhesions within cells were photobleached and allowed to recover for 90 s, either under shear or not. Shear was then applied (blue lines) or terminated (red lines) for 1 min and proximal adhesions were subsequently bleached and allowed to recover for a further 90 s. The percentage recovered GFP signal (i.e. the mobile fraction) for α5-integrin–GFP after each 90-s period is graphed. (C,D) B16F1 cells were transfected with α5-integrin–GFP, β1-integrin–GFP, or the G429N extended β1-integrin–GFP. For FRAP analysis, focal adhesions were photobleached under 20 dynes of shear or not. The percentage recovery of the GFP signal in the subsequent 90-s period is plotted. Each dot represents an individual ROI. k_{on} and k_{off} values that reflect the rates at which α5-integrin–GFP associated with and dissociated from focal adhesions were estimated from FRAP curves that were generated under no shear conditions. *P<0.01; ***P<0.001; NS, not significant (paired two-tailed Student's t-tests).

The form of cell–ECM adhesions can vary widely depending upon the cell type and the physical characteristics of the ECM they are attached to (Harunaga and Yamada, 2011). For example, increasing the stiffness of the ECM results in large stable focal adhesions, a phenomenon that is independent of increased integrin activation for ligand binding, implicating factors acting downstream of integrin engagement (Paszek et al., 2005; Tilghman et al., 2010). By examining cells attached to fibronectin where the intracellular tension was increased by shear stress, we were able to demonstrate that Rap1 activation is one such factor. Importantly, we also report that this post-adhesion function does not depend on the well-known ability of Rap1 to increase the affinity of integrins for ECM ligand (Boettner and Van Aelst, 2009).

Applied tension also stimulated the recruitment of vinculin to pre-existing adhesions. As this vinculin recruitment cascaded posteriorly from the leading edge of the cells under increased tension, and because it was both Rap dependent and negated by a short disruption of the actin cytoskeleton, we assessed the ability of Rap to affect actin dynamics at the leading edge of cells. We found that actin stability at the leading edge of the cell, as well as its retrograde flow back from that edge, was Rap dependent. Importantly, using RapL-GFP localization, we found that Rap activity overlapped with actin polymerization temporally at the leading edge. These results suggest that the ability of Rap to increase the stability of adhesions at the leading edge by recruiting vinculin is mediated by its effects on actin polymerization and retrograde flow there. Rap1 activation was also essential for establishing the polarity of Rac1 and PI3K activity at the leading edge. Therefore, it appears that Rap1 acts in a feed-forward loop to both initiate and reinforce leading-edge polarization under high-tension conditions that promote the initiation of tumor cell motility.

A number of studies have now shown that the application of tension regulates the residence time of molecular constituents of adhesions complexes (Dumbauld et al., 2013; Pines et al., 2012; Wolfenson et al., 2011). Collectively, these results have suggested that structural components of adhesions are stabilized, whereas regulatory adaptors and kinases have an increased exchange, in response to tension. Conversely, the reorientation of cells along the axis of tension necessitates the disassembly of preformed adhesions that are out of alignment. As tumor cells expressing a constitutively active form of Rap1 still elongated in the axis of tension in our studies, we surmise that the disassembly of preformed adhesions outside the axis of tension is Rap independent. Waterman and colleagues have implicated the activation of Src family kinases, focal adhesion kinase and calpain 2 in this action (Chen et al., 2013).

By altering matrix cross-linking *in vivo* and *in vitro* it has been determined that tumor cell growth, like invasion, is also a mechanosensitive phenomenon, at least for certain tumor types (Levental et al., 2009; Tilghman et al., 2010). Consistent with the finding that Rap1 activation regulated focal adhesion formation and invasion in 3D, activated Rap1 increased cell growth in low tension or on compliant matrices (e.g. non-crosslinked collagen gels) and increased subcutaneous tumor cell growth *in vivo*. In contrast, Rap activation had little effect on the growth of cells plated on rigid tissue culture plastic, which are already under high tension. This was all shown using a melanoma cell line, a cancer whose proliferation is not necessarily linked to stromal stiffness. It is interesting to note that increased Rap activation by either the increased expression of Rap or Rap-specific GEFs, or the decreased expression of Rap-specific GAPs, is found in many cancer types without known links to stromal stiffening. For example, the promoter region of Rap1GAP is frequently hypermethylated, leading to decreased Rap1GAP expression and increased Rap activation in thyroid cancers (Zuo et al., 2010), kidney cancers (Kim et al., 2012), squamous cell carcinomas of the head and neck (Banerjee et al., 2011), and melanomas (Zheng et al., 2009). In all of these cases, the increased Rap activation correlates with enhanced proliferation. Thus, in the absence of stromal stiffening, it appears that certain tumor types might subvert signaling pathways normally activated by tension in order to stimulate growth.

In vivo, the ECM crosslinking that increases tissue stiffness is slowly conditioned over the natural history of tumor development and progression (Levental et al., 2009). As such, much interest has been focused on the chronic tensional phenotype. Throughout the metastatic cascade, however, there might be abrupt changes in the microenvironmental tissue stiffness experienced by tumor cells

Journal of Cell Science (2017) 130, 152-163 doi:10.1242/jcs.180612

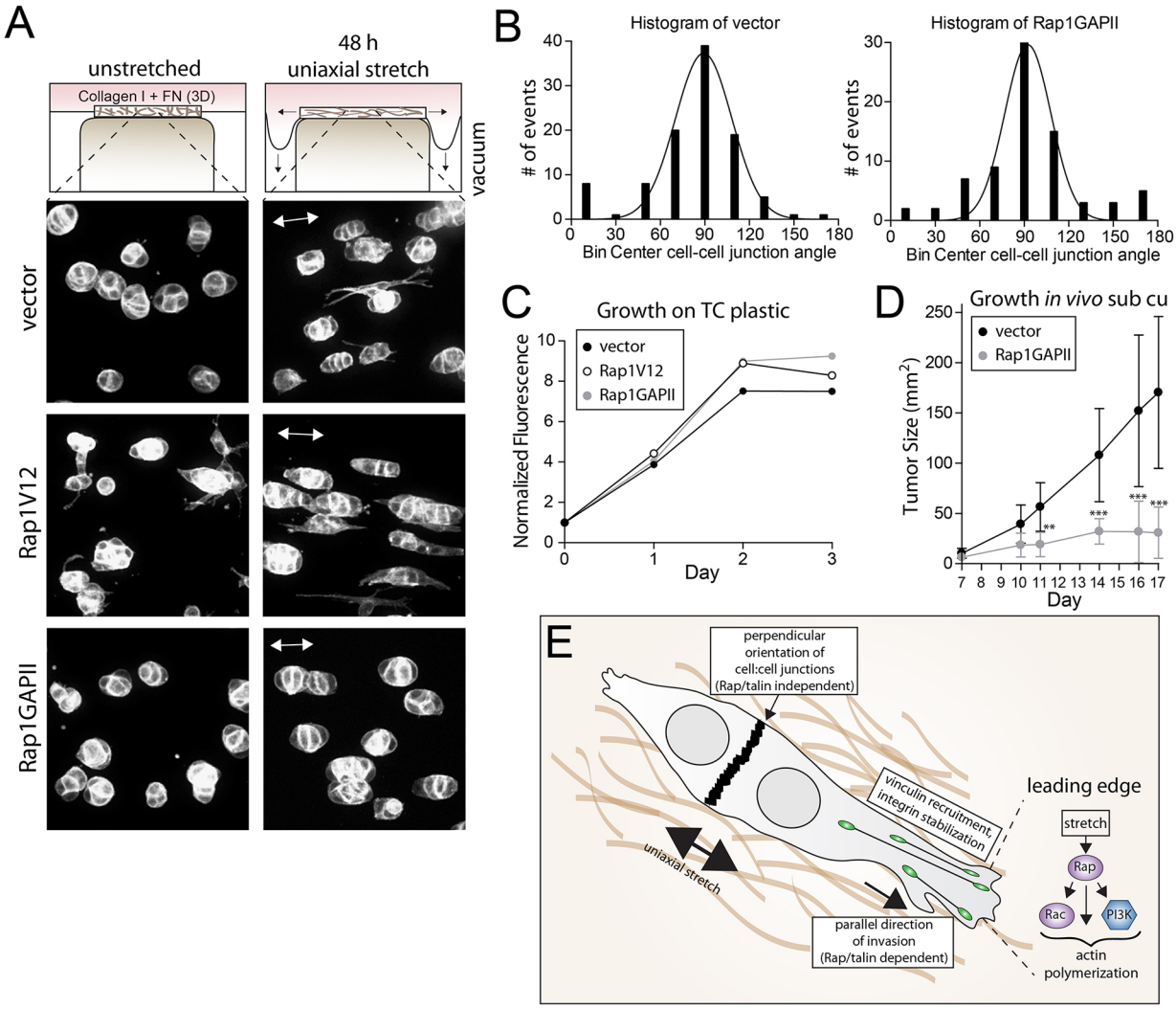

Fig. 7. Rap1-GTP regulates collective elongation of tumor cell clusters along the axis of tension as well as tumor growth *in vivo*. (A,B) Single B16F1 cells stably expressing a control vector, Rap1V12 or Rap1GAPII were seeded into collagen+fibronectin (FN) gels and grown for 48 h under uniaxial stretch. Arrows indicate the orientation of the applied tension. F-actin was stained (A) and the orientation of cell-cell junctions was determined for >75 cell clusters from three experiments (B). (C) Cells (1000/well) were seeded into 96-well plates in triplicate. Alamar Blue was added 4 h prior to each time point and, for each cell population, values were normalized to the day 0 value, which was defined as 1. The means from three independent experiments are graphed. (D) 1×10^5 cells were injected subcutaneously into C57Bl/6 mice and tumor sizes were quantified on the indicated days over a 17 day period. The mean±s.d. of tumor sizes from >20 mice from three separate experiments are graphed. $^{**}P<0.005$, $^{***}P<0.001$ (two-tailed paired Student's *t*-tests). (E) Model for Rap-dependent and -independent responses to applied tension.

(Kumar and Weaver, 2009). For example, upon seeding secondary organs, tumor cells might go from a stiff environment at the primary tumor to a compliant matrix within the perivascular niche at the distant site (Ghajar et al., 2013). The accumulation of mutations that lead to an intrinsic activation of mechanotransduction pathways might therefore augment late steps in metastasis, as would be the case with decreased expression of Rap-specific GAPs or increased expression of Rap-specific GEFs. Therefore, going forward it will be interesting to determine whether the dysregulation of tensional 'rheostats' is commonly selected for in tumor cells that colonize secondary organs, and whether this depends on the elastic modulus of microenvironment at the distant site.

MATERIALS AND METHODS

Cell lines

Eph4 cells were from John Muschler, Oregon Health and Science University (Portland, OR). EpRas and EpRasXT cells were from Hartmug Beug, Research Institute for Molecular Pathology, Vienna, Austria. MCF10a, MCF7, MDA-MB-231, and B16F1 cells were obtained from American Type Culture Collection (ATCC). B16F1 melanoma cells were stably co-transfected with either the pIRM21-IRES-dsFP593 empty vector or vectors driving the expression of FLAG–Rap1V12 or FLAG–Rap1GAPII constructs from Michiyuki Matsuda (Kyoto University, Kyoto, Japan) and pMSCVpuro (BD Clontech, CA) (Freeman et al., 2010). Cells were cultured in Dulbecco's Modified Eagle Medium (DMEM) supplemented with 8% fetal bovine serum (FBS) at 5% CO_2 and 37°C.

Transient transfections

Cells were transiently transfected using Lipofectamine 2000 (Invitrogen). α5-integrin–GFP and Raichu Rac1 FRET plasmids were from Robert Nabi (University of British Columbia, Vancouver, Canada). Akt (PH)–GFP was from Sergio Grinstein (The Hospital for Sick Children, Toronto, Canada). Rap1N17-Myc was from Michiyuki Matsuda. β1 integrin plasmids were from Valerie Weaver (University of California, San Francisco, CA). Rap1a (L-057058-01-0005) and Rap1b (L-062638-01-0005) siRNAs were

obtained from ThermoFisher Scientific. Tln1 (s75202) and Tln2 (s88928) siRNAs were purchased from Invitrogen. All siRNAs were used at a final concentration of 40 nM.

Uniaxial stretch of cells in 3D collagen

Collagen matrices were pre-assembled for 1 h on ice by mixing 10× DMEM with rat collagen I (5 mg/ml; BD Biosciences) at a ratio of 1:9 and adjusting the mixture to pH 7 using 1 N NaOH. Fibronectin (Sigma, 50 µg/ml final concentration) was added to pre-assembled collagen and mixed 1:1 with tumor cells (5×10^4 cells/ml final cell concentration, 2.17 µg/ml final collagen concentration). Tissue Train® Culture Plates (Flexcell International Corporation) were loaded onto Tissue Train® Linear Trough Loaders under 15% vacuum to create a linear trough. The matrix (120 µl) with embedded cells was loaded into troughs and allowed to polymerize for 2 h at 37°C. Medium (3 ml) was added to each well and cells were cultured overnight at 37°C prior to stretching. Plates were placed onto Arctangle® Loading Posts. A 46.55-kPa pressure was applied through the vacuum, pulling down the flexible-membrane where mesh was connected to the gel in order to create a 10% uniaxial elongation. Cells were fixed after 24–48 h of stretch.

Equibiaxial stretch of cells on 2D fibronectin-coated silicone rubber

Cells were detached using an enzyme-free cell dissociation buffer and 6.4×10^4 cells were seeded onto a six-well flexible silicone-bottom BioFlex® Culture Plate coated with 5 µg/cm^2 fibronectin. The cells were allowed to adhere for 4 h prior to the induction of stretch. Cells seeded on the flexible membrane culture plates were placed on the Bioflex 25-mm loading post. A 42.5 kPa vacuum pressure was applied to create an equibiaxial stretch of 10% on cells.

Immunofluorescence staining in 2D and 3D

Cells were fixed with 4% paraformaldehyde for 15 min, permeabilized with 0.1% Triton X-100 for 10 min and blocked with 10% normal goat serum (Jackson ImmunoResearch) in 1% BSA for 30 min. Cells were then stained for 1 h at room temperature (2D) or overnight at 4°C (3D) with a monoclonal anti-vinculin (1:100; cat. no. V4505, Sigma-Aldrich), anti-FLAG (1:200; cat. no. F7425, Sigma-Aldrich), and anti-β1 integrin (1:100; cat. no. 553715, BD Biosciences) antibodies. The cells were subsequently stained with Alexa-Fluor-488-conjugated goat anti-mouse-IgG (1:100; cat. no. A11029), Alexa-Fluor-568-conjugated goat anti-rabbit-IgG (1:100; cat. no. A11011), or Alexa-Fluor-647-conjugated goat anti-rat-IgG (1:100; cat. no. A21247) secondary antibodies plus Rhodamine–phalloidin (1:200; cat. no. R415) all from Invitrogen for 1 h. The samples were then mounted using ProLong Gold containing DAPI (Molecular Probes). Cells in 3D matrices were visualized using a 25×1.45 NA or 100×1.45 NA objective on a Zeiss 200M Axiovert microscope. Intensities and volumes were analyzed using Slidebook v5.5 (3i Intelligent Imaging Innovations).

Fluorescence recovery after photobleaching

Regions of interest (ROIs) containing α5-integrin–GFP-positive focal adhesions were photobleached using a 405 nm laser (100% intensity, 0.1 s) on an Olympus FV1000 confocal microscope (Central Valley, PA). Fluorescence recovery was recorded at 4- or 5-s time intervals for 90 s. Olympus FluoView v1.6 software was used to quantify recovery of fluorescence signal, which is expressed as a percentage of the pre-bleach intensity. Single exponential fit curves of the fluorescence recovery data were generated using Prism 4 software. These curves were used to determine the k_{on} and k_{off} rates, as described previously (Pines et al., 2012).

Collagen gel contraction and growth assays

Collagen I and fibronectin matrices were prepared as described above and mixed 1:1 with B16F1 cells to yield final concentrations of 1.77 mg/ml collagen, 5 µg/ml fibronectin, and 10^5–10^6 cells/ml in a total volume of 200 µl. For contraction assays, the matrices with embedded cells were added to 12-well cell culture inserts (BD Falcon) with growth medium and incubated for 2 days prior to lifting the gel. Lifted gels were then allowed to contract overnight at 37°C and gel diameters were quantified the next day.

For growth assays, after 5 days in culture, the cells were fixed and visualized using the 20× objective lens on a Zeiss 200M Axiovert microscope. Focal adhesion and actin staining were visualized using a 100×1.45 NA objective. Volumetric analysis was performed using Slidebook v5.5 (3i Intelligent Imaging Innovations).

Rac1 and RhoA G-LISA

B16F1 cells were seeded at a density of 1.5×10^5 cells per well and then cultured overnight in six-well silicone rubber BioFlex® Culture Plates (Flexcell International Corporation, Hillsborough, CA) that had been coated with 5 µg/cm^2 fibronectin. A 10% equibiaxial mechanical stretch was applied for 2–30 min. Rac1- and RhoA-specific G-LISAs were performed according to the manufacturer's instructions (Cytoskeleton).

Immunoblotting

Cells were lysed in RIPA buffer containing protease and phosphatase inhibitors.

After separating proteins by SDS-PAGE and transferring onto PVDF membranes, the membranes were blocked with 5% BSA for 1 h at room temperature and then incubated overnight at 4°C with primary antibodies diluted in 1% BSA. The antibodies used were: from Santa Cruz Biotechnology, anti-Rap1 (1:1000, cat no. sc-28197) and anti-talin (1:1000, cat. no. sc-7534, Santa Cruz); from Invitrogen, anti-Rap2 (1:1000, cat no. ab173296); from Sigma, anti-vinculin (1:2000, cat. no. V4505), anti-FLAG (1:10,000, cat. no. F7425) and anti-β-actin (1:5000, cat. no. A4700); from Cell Signaling Technologies, anti-pY165-p130Cas (1:1000, cat. no. 4015), anti-p130Cas (1:1000, cat. no. 13846), anti-pS19 myosin light chain II (1:1000, cat no. 3671P); and from Abcam, anti-pY118 paxillin (1:1000, cat no. 44-722G). Membranes were then incubated with the appropriate horseradish peroxidase (HRP)-conjugated secondary antibody diluted in 1% BSA for 1 h at room temperature and bands were visualized using Immobilon Western Chemiluminescent HRP Substrate (Millipore).

Competing interests

The authors declare no competing or financial interests.

Author contributions

S.A.F., S.T., D.C., M.R.G, and C.D.R conceived and designed experimental systems; S.A.F, S.C., P.A., I.I., M.L.G., and L.H. performed experiments; S.A.F, S.C., P.A., I.I., and M.L.G. analysed the data; S.A.F., S.C., P.A., M.R.G., and C.D.R. wrote the manuscript.

Funding

This work was supported by grants from the Canadian Institutes of Health Research [grant number MOP-10463 to M.R.G. and C.D.R.]; and the Natural Sciences and Engineering Research Council of Canada [grant number RGPIN-1501-04611 to D.C.].

Supplementary information

Supplementary information available online at
http://jcs.biologists.org/lookup/doi/10.1242/jcs.180612.supplemental

References

Abiko, H., Fujiwara, S., Ohashi, K., Hiatari, R., Mashiko, T., Sakamoto, N., Sato, M. and Mizuno, K. (2015). Rho guanine nucleotide exchange factors involved in cyclic-stretch-induced reorientation of vascular endothelial cells. *J. Cell Sci.* **128**, 1683-1695.

Balachandran, K., Alford, P. W., Wylie-Sears, J., Goss, J. A., Grosberg, A., Bischoff, J., Aikawa, E., Levine, R. A. and Parker, K. K. (2011). Cyclic strain induces dual-mode endothelial-mesenchymal transformation of the cardiac valve. *Proc. Natl. Acad. Sci. USA* **108**, 19943-19948.

Banerjee, R., Mani, R.-S., Russo, N., Scanlon, C. S., Tsodikov, A., Jing, X., Cao, Q., Palanisamy, N., Metwally, T., Inglehart, R. C. et al. (2011). The tumor suppressor gene rap1GAP is silenced by miR-101-mediated EZH2 overexpression in invasive squamous cell carcinoma. *Oncogene* **30**, 4339-4349.

Boettner, B. and Van Aelst, L. (2009). Control of cell adhesion dynamics by Rap1 signaling. *Curr. Opin Cell Biol.* **5**, 684-693.

Boettner, B., Govek, E.-E., Cross, J. and Van Aelst, L. (2000). The junctional multidomain protein AF-6 is a binding partner of the Rap1A GTPase and associates with the actin cytoskeletal regulator profilin. *Proc. Natl. Acad. Sci. USA* **97**, 9064-9069.

Bos, J. L. (2005). Linking Rap to cell adhesion. *Curr. Opin. Cell Biol.* **17**, 123-128.

Bravo-Cordero, J. J., Magalhaes, M. A. O., Eddy, R. J., Hodgson, L. and Condeelis, J. (2013). Functions of cofilin in cell locomotion and invasion. *Nat. Rev. Mol. Cell Biol.* **14**, 405-415.

Bronsert, P., Enderle-Ammour, K., Bader, M., Timme, S., Kuehs, M., Csanadi, A., Kayser, G., Kohler, I., Bausch, D., Hoeppner, J., Hopt, U. T., Keck, T., Stickeler, E., Passlick, B., Schilling, O., Reiss, C. P., Vashist, Y., Brabletz, T., Berger, J., Lotz, J., Olesch, J., Werner, M., Wellner, U. F. (2014). Cancer cell invasion and EMT marker expression: a three-dimensional study of the human cancer–host interface. *J Pathol.* **234**, 410-422.

Chen, Y., Pasapera, A. M., Koretsky, A. P. and Waterman, C. M. (2013). Orientation-specific responses to sustained uniaxial stretching in focal adhesion growth and turnover. *Proc. Natl. Acad. Sci. USA* **110**, E2352-E2361.

Collins, C., Guilluy, C., Welch, C., O'Brien, E. T., Hahn, K., Superfine, R., Burridge, K. and Tzima, E. (2012). Localized tensional forces on PECAM-1 elicit a global mechanotransduction response via the integrin-RhoA pathway. *Curr. Biol.* **22**, 2087-2094.

de Bruyn, K. M. T., Zwartkruis, F. J. T., de Rooij, J., Akkerman, J.-W. N. and Bos, J. L. (2003). The small GTPase Rap1 is activated by turbulence and is involved in integrin alpha(IIb)beta(3)-mediated cell adhesion in human megakaryocytes. *J. Biol. Chem.* **278**, 22412-22417.

del Rio, A., Perez-Jimenez, R., Liu, R., Roca-Cusachs, P., Fernandez, J. M. and Sheetz, M. P. (2009). Stretching single talin rod molecules activates vinculin binding. *Science* **323**, 638-641.

Dumbauld, D. W., Lee, T. T., Singh, A., Scrimgeour, J., Gersbach, C. A., Zamir, E. A., Fu, J., Chen, C. S., Curtis, J. E., Craig, S. W. et al. (2013). How vinculin regulates force transmission. *Proc. Natl. Acad. Sci. USA* **110**, 9788-9793.

Fraley, S. I., Feng, Y., Krishnamurthy, R., Kim, D.-H., Celedon, A., Longmore, G. D. and Wirtz, D. (2010). A distinctive role for focal adhesion proteins in three-dimensional cell motility. *Nat. Cell Biol.* **12**, 598-604.

Freeman, S. A., McLeod, S. J., Dukowski, J., Austin, P., Lee, C. C. Y., Millen-Martin, B., Kubes, P., McCafferty, D.-M., Gold, M. R. and Roskelley, C. D. (2010). Preventing the activation or cycling of the Rap1 GTPase alters adhesion and cytoskeletal dynamics and blocks metastatic melanoma cell extravasation into the lungs. *Cancer Res.* **70**, 4590-4601.

Freeman, S. A., Lei, V., Dang-Lawson, M., Mizuno, K., Roskelley, C. D. and Gold, M. R. (2011). Cofilin-mediated F-actin severing is regulated by the Rap GTPase and controls the cytoskeletal dynamics that drive lymphocyte spreading and BCR microcluster formation. *J. Immunol.* **187**, 5887-5900.

Geiger, B. and Yamada, K. M. (2011). Molecular architecture and function of matrix adhesions. *Cold Spring Harb. Perspect. Biol.* **3**, a005033.

Ghajar, C. M., Peinado, H., Mori, H., Matei, I. R., Evason, K. J., Brazier, H., Almeida, D., Koller, A., Hajjar, K. A., Stainier, D. Y. R. et al. (2013). The perivascular niche regulates breast tumour dormancy. *Nat. Cell Biol.* **15**, 807-817.

Goetz, J. G., Minguet, S., Navarro-Lérida, I., Lazcano, J. J., Samaniego, R., Calvo, E., Tello, M., Osteso-Ibáñez, T., Pellinen, T., Echarri, A. et al. (2011). Biomechanical remodeling of the microenvironment by stromal caveolin-1 favors tumor invasion and metastasis. *Cell* **146**, 148-163.

Grashoff, C., Hoffman, B. D., Brenner, M. D., Zhou, R., Parsons, M., Yang, M. T., McLean, M. A., Sligar, S. G., Chen, C. S., Ha, T. et al. (2010). Measuring mechanical tension across vinculin reveals regulation of focal adhesion dynamics. *Nature* **466**, 263-266.

Hahn, C., Wang, C., Orr, A. W., Coon, B. G. and Schwartz, M. A. (2011). JNK2 promotes endothelial cell alignment under flow. *PLoS ONE* **6**, e24338.

Han, J., Lim, C. J., Watanabe, N., Soriani, A., Ratnikov, B., Calderwood, D. A., Puzon-McLaughlin, W., Lafuente, E. M., Boussiotis, V. A., Shattil, S. J. et al. (2006). Reconstructing and deconstructing agonist-induced activation of integrin alphaIIbbeta3. *Curr. Biol.* **16**, 1796-1806.

Harunaga, J. S. and Yamada, K. M. (2011). Cell-matrix adhesions in 3D. *Matrix Biol.* **30**, 363-368.

Kim, W.-J., Gersey, Z. and Daaka, Y. (2012). Rap1GAP regulates renal cell carcinoma invasion. *Cancer Lett.* **320**, 65-71.

Kortholt, A., Bolourani, P., Rehmann, H., Keizer-Gunnink, I., Weeks, G., Wittinghofer, A. and Van Haastert, P. J. M. (2010). A Rap/phosphatidylinositol 3-kinase pathway controls pseudopod formation. *Mol. Biol. Cell* **21**, 936-945.

Kumar, S. and Weaver, V. M. (2009). Mechanics, malignancy, and metastasis: the force journey of a tumor cell. *Cancer Metastasis Rev.* **28**, 113-127.

Lafuente, E. M., van Puijenbroek, A. A. F. L., Krause, M., Carman, C. V., Freeman, G. J., Berezovskaya, A., Constantine, E., Springer, T. A., Gertler, F. B. and Boussiotis, V. A. (2004). RIAM, an Ena/VASP and Profilin ligand, interacts with Rap1-GTP and mediates Rap1-induced adhesion. *Dev. Cell* **7**, 585-595.

Levental, K. R., Yu, H., Kass, L., Lakins, J. N., Egeblad, M., Erler, J. T., Fong, S. F. T., Csiszar, K., Giaccia, A., Weninger, W. et al. (2009). Matrix crosslinking forces tumor progression by enhancing integrin signaling. *Cell* **139**, 891-906.

Lu, P., Weaver, V. M. and Werb, Z. (2012). The extracellular matrix: a dynamic niche in cancer progression. *J. Cell Biol.* **196**, 395-406.

Mammoto, A., Huang, S., Moore, K., Oh, P. and Ingber, D. E. (2004). Role of RhoA, mDia, and ROCK in cell shape-dependent control of the Skp2-p27kip1 pathway and the G1/S transition. *J. Biol. Chem.* **279**, 26323-26330.

Margadant, F., Chew, L. L., Hu, X., Yu, H., Bate, N., Zhang, X. and Sheetz, M. (2011). Mechanotransduction in vivo by repeated talin stretch-relaxation events depends upon vinculin. *PLoS Biol.* **9**, e1001223.

Mouneimne, G., DesMarais, V., Sidani, M., Scemes, E., Wang, W., Song, X., Eddy, R. and Condeelis, J. (2006). Spatial and temporal control of cofilin activity is required for directional sensing during chemotaxis. *Curr. Biol.* **16**, 2193-2205.

Parri, M. and Chiarugi, P. (2010). Rac and Rho GTPases in cancer cell motility control. *Cell Commun. Signal.* **8**, 23.

Pasapera, A. M., Schneider, I. C., Rericha, E., Schlaepfer, D. D. and Waterman, C. M. (2010). Myosin II activity regulates vinculin recruitment to focal adhesions through FAK-mediated paxillin phosphorylation. *J. Cell Biol.* **188**, 877-890.

Paszek, M. J., Zahir, N., Johnson, K. R., Lakins, J. N., Rozenberg, G. I., Gefen, A., Reinhart-King, C. A., Margulies, S. S., Dembo, M., Boettiger, D. et al. (2005). Tensional homeostasis and the malignant phenotype. *Cancer Cell* **8**, 241-254.

Pines, M., Das, R., Ellis, S. J., Morin, A., Czerniecki, S., Yuan, L., Klose, M., Coombs, D. and Tanentzapf, G. (2012). Mechanical force regulates integrin turnover in Drosophila in vivo. *Nat. Cell Biol.* **14**, 935-943.

Provenzano, P. P. and Keely, P. J. (2011). Mechanical signaling through the cytoskeleton regulates cell proliferation by coordinated focal adhesion and Rho GTPase signaling. *J. Cell Sci.* **124**, 1195-1205.

Provenzano, P. P., Eliceiri, K. W., Campbell, J. M., Inman, D. R., White, J. G. and Keely, P. J. (2006). Collagen reorganization at the tumor-stromal interface facilitates local invasion. *BMC Med.* **4**, 38.

Raaijmakers, J. H. and Bos, J. L. (2009). Specificity in Ras and Rap Signaling. *J. Biol. Chem.* **284**, 10995-10999.

Riveline, D., Zamir, E., Balaban, N. Q., Schwarz, U. S., Ishizaki, T., Narumiya, S., Kam, Z., Geiger, B. and Bershadsky, A. D. (2001). Focal contacts as mechanosensors: externally applied local mechanical force induces growth of focal contacts by an mDia1-dependent and ROCK-independent mechanism. *J. Cell Biol.* **153**, 1175-1186.

Rubashkin, M. G., Cassereau, L., Bainer, R., DuFort, C. C., Yui, Y., Ou, G., Paszek, M. J., Davidson, M. W., Chen, Y.-Y. and Weaver, V. M. (2014). Force engages vinculin and promotes tumor progression by enhancing PI3K activation of phosphatidylinositol (3,4,5)-triphosphate. *Cancer Res.* **74**, 4597-4611.

Sawada, Y., Tamada, M., Dubin-Thaler, B. J., Cherniavskaya, O., Sakai, R., Tanaka, S. and Sheetz, M. P. (2006). Force sensing by mechanical extension of the Src family kinase substrate p130Cas. *Cell* **127**, 1015-1026.

Tamada, M., Sheetz, M. P. and Sawada, Y. (2004). Activation of a signaling cascade by cytoskeleton stretch. *Dev. Cell* **7**, 709-718.

Thery, M. and Bornens, M. (2006). Cell shape and cell division. *Curr. Opin. Cell Biol.* **18**, 648-657.

Thery, M., Racine, V., Pepin, A., Piel, M., Chen, Y., Sibarita, J.-B. and Bornens, M. (2005). The extracellular matrix guides the orientation of the cell division axis. *Nat. Cell Biol.* **7**, 947-953.

Thievessen, I., Thompson, P. M., Berlemont, S., Plevock, K. M., Plotnikov, S. V., Zemljic-Harpf, A., Ross, R. S., Davidson, M. W., Danuser, G., Campbell, S. L. et al. (2013). Vinculin-actin interaction couples actin retrograde flow to focal adhesions, but is dispensable for focal adhesion growth. *J. Cell Biol.* **202**, 163-177.

Tilghman, R. W., Cowan, C. R., Mih, J. D., Koryakina, Y., Gioeli, D., Slack-Davis, J. K., Blackman, B. R., Tschumperlin, D. J. and Parsons, J. T. (2010). Matrix rigidity regulates cancer cell growth and cellular phenotype. *PLoS ONE* **5**, e12905.

Tzima, E., Irani-Tehrani, M., Kiosses, W. B., Dejana, E., Schultz, D. A., Engelhardt, B., Cao, G., DeLisser, H. and Schwartz, M. A. (2005). A mechanosensory complex that mediates the endothelial cell response to fluid shear stress. *Nature* **437**, 426-431.

Wojciak-Stothard, B. and Ridley, A. J. (2003). Shear stress-induced endothelial cell polarization is mediated by Rho and Rac but not Cdc42 or PI 3-kinases. *J. Cell Biol.* **161**, 429-439.

Wolfenson, H., Bershadsky, A., Henis, Y. I. and Geiger, B. (2011). Actomyosin-generated tension controls the molecular kinetics of focal adhesions. *J. Cell Sci.* **124**, 1425-1432.

Zheng, H., Gao, L., Feng, Y., Yuan, L., Zhao, H. and Cornelius, L. A. (2009). Down-regulation of Rap1GAP via promoter hypermethylation promotes melanoma cell proliferation, survival, and migration. *Cancer Res.* **69**, 449-457.

Zuo, H., Gandhi, M., Edreira, M. M., Hochbaum, D., Nimgaonkar, V. L., Zhang, P., DiPaola, J., Evdokimova, V., Altschuler, D. L. and Nikiforov, Y. E. (2010). Downregulation of Rap1GAP through epigenetic silencing and loss of heterozygosity promotes invasion and progression of thyroid tumors. *Cancer Res.* **70**, 1389-1397.

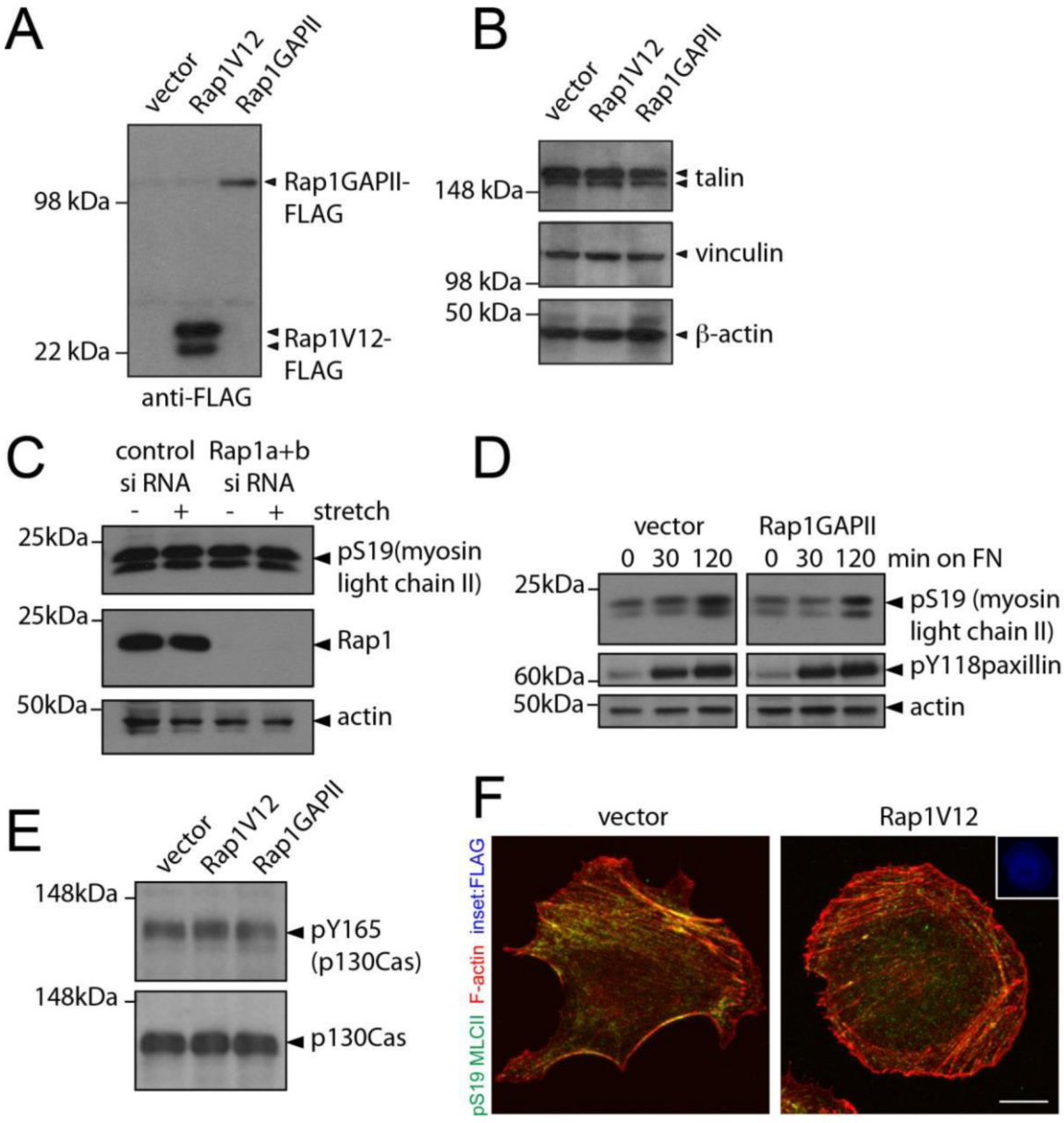

Figure S1 (relates to Figure 3 and 4). Rap activation does not alter the expression of focal adhesion proteins nor regulate the phosphorylation of myosin light chain II, paxillin, or p130Cas. A-B) B16F1 cells stably expressing vector, Rap1V12, and Rap1GAPII were lysed and probed with indicated antibodies. C) B16F1 cells were transfected with control or si RNA directed against Rap1a and Rap1b. Cells were seeded onto FN (5 μg/cm^2) coated silicone rubber plates overnight before applying 10% equibiaxial stretch to the substrata for 5 min, lysed, and probed with indicated antibodies. D) B16F1 cells expressing vector control or Rap1GAPII were seeded onto FN (5 μg/cm^2) coated tissue culture plates for indicated times, lysed, and probed with indicated antibodies. E) B16F1 cells were seeded onto FN (5 μg/cm^2) coated silicone rubber plates overnight before applying 10% equibiaxial stretch to the substrata for 5 min, lysed, and probed with indicated antibodies. F) B16F1 cells were seeded onto FN (5 μg/cm^2) coated coverglass for 2 h, fixed, and stained for pS19MLCII and F-actin. Scale bar, 10 μm.

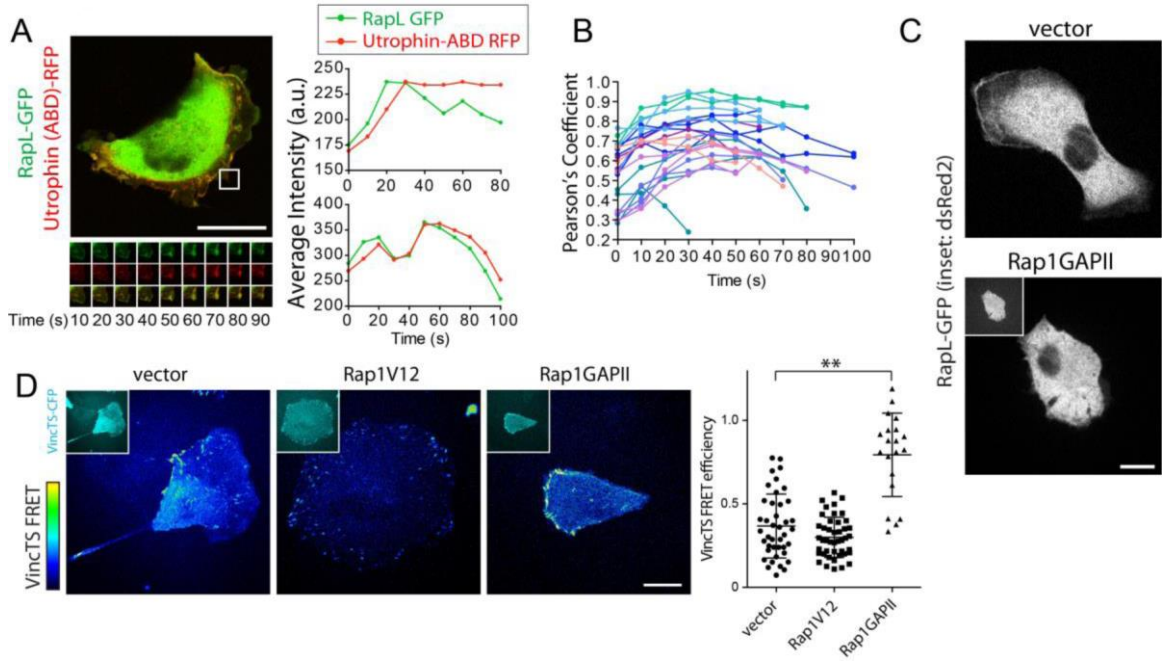

Figure S2 (relates to Figure 4). Active Rap localizes to the leading edge and regulates tension through vinculin. A-B) B16F1 cells transfected with RapL-GFP and the actin-binding domain (ABD) of utrophin fused to RFP were imaged on FN (2.5 μg cm^{-2}) coated chamber slides. As new membrane ruffling events occurred, RapL-GFP and utrophin (ABD)-RFP fluorescence were recorded. For a representative cell, time-dependent changes in RapL-GFP and utrophin (ABD)-RFP intensities within a region of interest (ROI) at the leading edge (white box) are graphed, middle panel. The Pearson's coefficient for >20 leading edge ROIs from 5 cells with active membrane ruffling are shown (B). Scale bar: 20 μm. C) B16F1 cells transfected with RapL-GFP and Rap1GAPII in a vector containing dsRed2 were imaged on FN (2.5 μg cm^{-2}) coated chamber slides. Note that the localization of RapL-GFP to the plasma membrane requires Rap activation. D) B16F1 cells were transiently transfected with vector, Rap1GAPII-FLAG, or Rap1V12 along with the vinculin tension sensor (VincTS). A ratio of the CFP signal before and after bleaching YFP for 3 frames is shown. N > 20 cells from 3 experiments. All scale bars are 20 μm. Significance was calculated using Student's unpaired two-tailed t-tests (**P < 0.01).

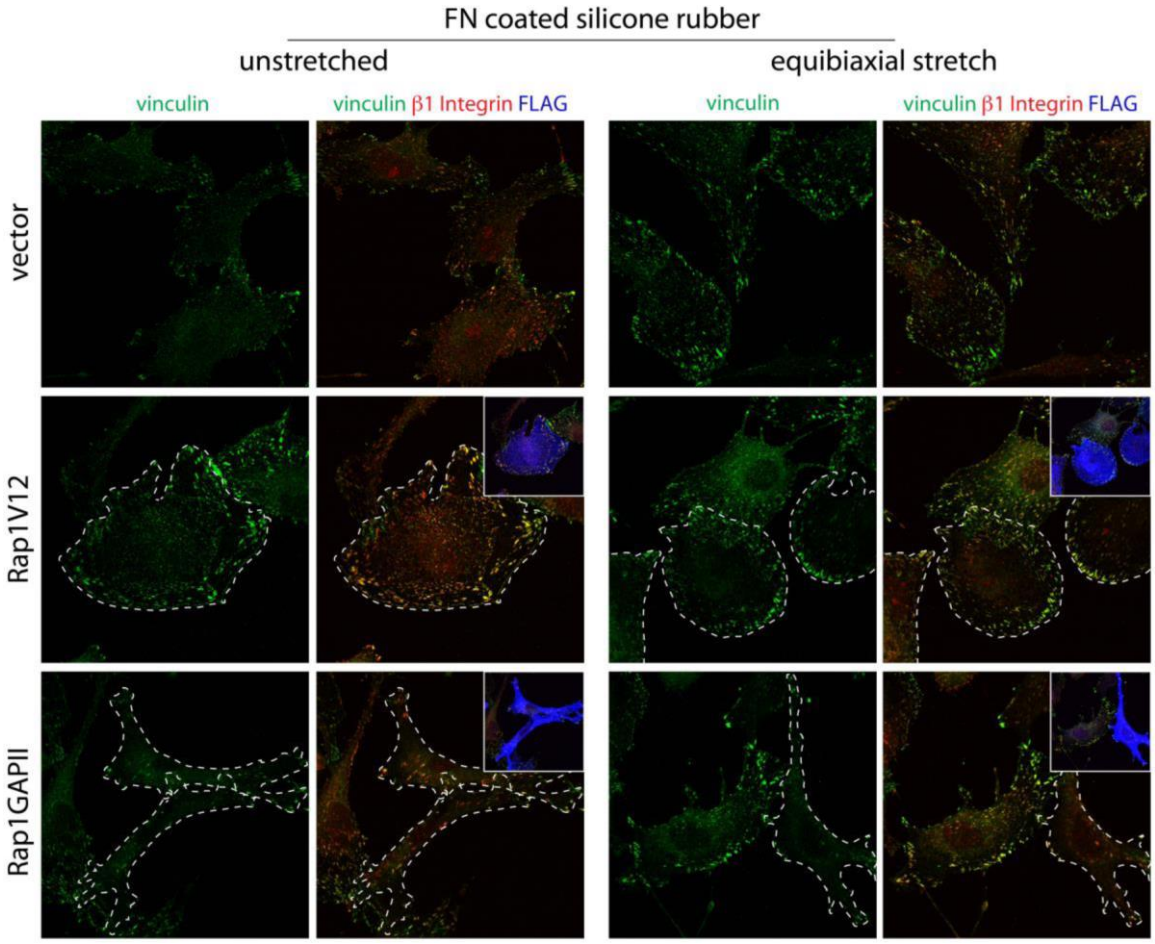

Supplementary Figure 3 (relates to Figure 4). Vinculin enrichment at focal adhesions in response to stretch in 2D. B16F1 cells transiently expressing vector, Rap1V12-FLAG, or Rap1GAPII-FLAG were seeded onto FN (2.5 μg cm^{-2}) coated silicone rubber plates overnight before applying 10% equibiaxial stretch to the substrata for 4 h. Cells were fixed and stained for vinculin and β1-integrin.

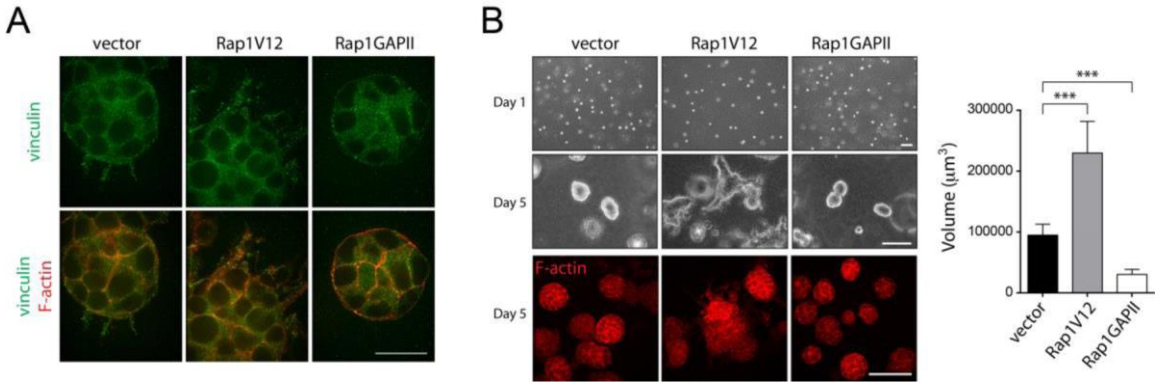

Supplemental Figure 4 (relates to Figure 7). Rap1-GTP regulates growth in 3D collagen gels. A-B) Single B16F1 cells stably expressing a control vector, Rap1V12, or Rap1GAPII were seeded into collagen + FN gels and grown for 5 days. A) Vinculin and F-actin were stained and the border of individual colonies with the matrix is shown. Scale bar: 100 μm. B) Phase contrast and F-actin imaging of individual fields at days 1 and 5 (left). F-actin staining was used to determine colony volume (right). Scale bar: 500 μm. *** P<0.001.